Autonomous Operation of Hybrid Microgrid With AC and DC Subgrids

Poh Chiang Loh, *Senior Member, IEEE*, Ding Li, Yi Kang Chai, and Frede Blaabjerg, *Fellow, IEEE*

***Abstract*—This paper investigates on power-sharing issues of an autonomous hybrid microgrid. Unlike existing microgrids which are purely ac, the hybrid microgrid studied here comprises dc and ac subgrids interconnected by power electronic interfaces. The main challenge here is to manage power flows among all sources distributed throughout the two types of subgrids, which is certainly tougher than previous efforts developed for only ac or dc microgrid. This wider scope of control has not yet been investigated, and would certainly rely on the coordinated operation of dc sources, ac sources, and interlinking converters. Suitable control and normalization schemes are now developed for controlling them with the overall hybrid microgrid performance already verified in simulation and experiment.**

***Index Terms*—AC microgrids, active power sharing, dc microgrids, droop control, hybrid microgrids.**

I. Introduction

ADVANTAGES such as environmental friendliness, expandability, and flexibility have made distributed generation (DG), powered by various renewable and nonconventional microsources, an attractive option for configuring modern electrical grids [1], [2]. When a few distributed sources and loads are further clustered together, entities known as microgrids are formed, which are, in principle, larger controllable distributed generators that merge advantages of various nonconventional sources [3]–[5]. Accompanying this advancement in DG and microgrids is the development of various essential power conditioning interfaces and their associated control for tying multiple microsources to the microgrids, and then tying the microgrids to the traditional power systems. With such interconnection, microgrid operation is highly flexible, allowing it to operate freely in the grid-connected or islanded mode of operation [1]–[5]. For the former, each microsource can be operated like a current source with maximum power transferred to the grid. That is possible only when the grid is much larger in capacity, and can hence be treated as an infinite bus.

In contrast, if the mains grid is not comparatively larger or is simply disconnected due to the occurrence of a fault, the islanded mode of operation with more stringent supply–demand balancing requirements will be triggered. Without a strong grid and a firm system voltage, each microsource must now regulate its own terminal voltage within an allowed range determined by its internally generated reference [6]–[9]. The microsource thus appears like a controlled voltage source, whose output should rightfully share the load demand with the other sources. The sharing should preferably be in proportion to their power ratings so as not to overstress any individual entity. It should also be achieved with no or minimal communication link that is not detrimental to the overall system operation if it fails. This is important since most microsources are widely dispersed, and hence impractical to link by wires. Avoiding the wiring would then constrain measurements to be taken only within the local vicinity of each microsource. So far, this can only be met by the droop control method, where virtual inertia is intentionally added to each microsource [6]–[10].

Most existing droop control techniques, however, concentrate only on DG control in ac microgrids [6]–[16], which is understandable judging from the dominant role that ac distribution serves in traditional grids. Although much rarely seen, droop control applied to dc microgrids is also possible, and has in fact been discussed more than a decade back in [17]. Its study has not grown since then even though there are a few recent references discussing about dc grids, but not really their droop control [18]–[25]. Interest in dc microgrids might grow soon though due to the proliferation of photovoltaic (PV) generation, fuel cells, and energy storages such as batteries and other capacitive alternatives, which are dc by nature. Moreover, modern high-tech loads are mostly electronic circuits that need dc rather than ac supply, hence raising the attractiveness of dc microgrids, which need lesser power conversion stages in general.

Having dc microgrids alone is, however, not realistic, since as mentioned earlier, ac distribution is presently dominant, and would be so for many more decades. Therefore, a more likely scenario would be the presence of both dc and ac subgrids with sources, storages, and loads appropriately distributed between them. The subgrids can subsequently be tied together by interlinking converters to form hybrid ac–dc microgrid. The accompanied challenge is then to design a coordinated droop control scheme for controlling the hybrid microgrid so that power is shared among the sources in proportion to their power ratings rather than physical placements within the hybrid microgrid.

Manuscript received December 30, 2011; revised March 14, 2012; accepted July 26, 2012. Date of current version November 22, 2012. This paper was presented at Europe Power Electronics and Adjustable Speed Drives, Birmingham, U.K., August 30–September 1, 2011. This work was supported by the Agency for Science, Technology and Research (A∗Star), Singapore, under the Intelligent Energy Distribution Systems program. Recommended for publication by Associate Editor B. Ozpineci.

P. C. Loh is with the School of Electrical and Electronic Engineering, Nanyang Technological University, 639798 Singapore (e-mail: epcloh@ntu.edu.sg).

D. Li is with the WERL Laboratory, School of Electrical and Electronic Engineering, Nanyang Technological University, 639798 Singapore (e-mail: e080010@ntu.edu.sg).

Y. K. Chai is with SP PowerGrid Limited, Mapletree Business City, 117438 Singapore (e-mail: chai0054@ntu.edu.sg).

F. Blaabjerg is with the Department of Energy Technology, Aalborg University, 9220 Aalborg, Denmark (e-mail: fbl@et.aau.dk).

Color versions of one or more of the figures in this paper are available online at http://ieeexplore.ieee.org.

Digital Object Identifier 10.1109/TPEL.2012.2214792

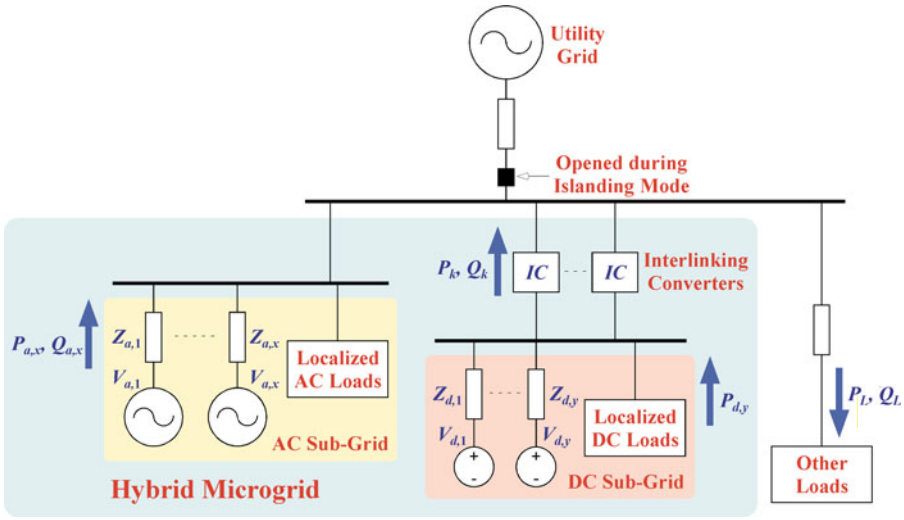

Fig. 1. Example hybrid microgrid.

Such sharing can only be enforced by controlling the interlinking converters to transfer the right amount of energy between the two types of subgrids, whose value is decided by the designed droop control scheme. This effort has not been previously pursued by other researchers, and is now discussed for various hybrid microgrid architectural layouts. It is important to clarify here too that this paper is an extension of [26] written by the authors. Some concepts that have not been appropriately discussed in [26] are now explained with better clarity.

II. System Structure

Fig. 1 shows an example hybrid microgrid formed by a dc subgrid and an ac subgrid. Each subgrid has its own sources, storages, and loads of the same type grouped together so as to minimize the amount of power conversion needed. Between the subgrids can either be one or multiple interlinking converters, depending on their ratings and those of the subgrids. Regardless of their number though, the role of the interlinking converters is to provide bidirectional energy transfer between the subgrids, depending on their prevailing internal supply–demand conditions. The formed hybrid microgrid can then be tied to the ac utility mains through an intelligent transfer switch like with other ac microgrids. This switch will stay on under normal grid-connected mode of operation, and if the mains is strong with sizable capacity, maximum energy from the hybrid microgrid can be harnessed with any surplus injected or shortfall absorbed from the mains. Supply–demand balancing within the microgrid is, therefore, less stringent with the mains effectively behaving like an infinite bus. Its control is, therefore, less involved with sources and storages in both subgrids operating independently at their maximum or optimal power points without referring to the statuses of others.

If an upstream fault is now sensed from the mains, the transfer switch will break to form an autonomous island isolated from the mains. Islanding should rightfully have more complex supply–demand considerations since the infinite mains is no longer there to cushion any unbalance. That also means sources can no longer produce maximum or optimal powers continuously if the combined capacity of the loads and storages is not capable of absorbing the full amount of power generated. Some knowledge of the load and storage charging demand is, therefore, needed, and should be communicated to all sources. The sources, being properly informed, can then decide on the right amount of energy to produce that would meet the demand, while yet not overstressing themselves. The sharing of information can certainly be realized by adding an explicit communication link, together with its accompanied costs, which probably might create a single point of failure. To avoid such addition, droop control can be considered, where each source is responsible to sense its terminal load demand, and share it with others by adjusting its terminal voltage magnitude, frequency, and phase [6]–[16]. Upon reaching steady state, the sources would have finished their "negotiation" with each of them producing a fraction of the demand in proportion to its power rating. Explicit communication link is, therefore, not needed since information has already been indirectly "communicated" by adjusting the parameters of the existing power network.

Presently, droop control is well established with many variants proposed in the literature, but mainly for an ac microgrid [6]–[16]. Its extension to a hybrid microgrid has not been previously investigated, and would generally be more complex since it spans across at least two subgrids of either ac or dc form. The challenges would mostly be with the control of the single or multiple interlinking converters shown in Fig. 1 and discussed in a later section.

III. Autonomous Control Within Subgrids

Control of a hybrid microgrid can be managed by first viewing at the control of its individual subgrids, before discussing about their coordination upon being tied by interlinking converters. This section, therefore, begins with a review of droop control applied to an ac subgrid before shifting the concepts to a dc subgrid. Control of interlinking converters to coordinate the

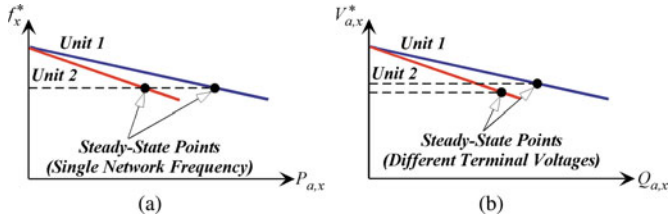

Fig. 2. Active and reactive power droop characteristics for an ac subgrid.

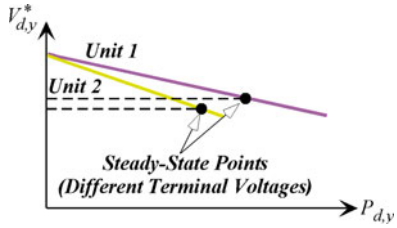

Fig. 3. Active power droop characteristic for a dc subgrid.

two subgrids follows in the next section, which conceptually is the main challenge and contribution of this paper.

A. Droop Control for an AC Subgrid

Droop control applied to an ac subgrid with at least two paralleled sources has widely been investigated like in [6]–[16]. Each source, in principle, uses two droop control equations for determining its reference frequency f and voltage amplitude V_a from its locally measured active P_a and reactive Q_a power values, respectively. If subscript x is used for representing the source index in the ac subgrid, the two droop equations assigned to unit x can appropriately be written as

$$f_x^* = f_x' + m_x P_{a,x}; \quad V_{a,x}^* = V_{a,x}' + n_x Q_{a,x} \tag{1}$$

where f_x' and $V_{a,x}'$ are the maximum frequency and voltage amplitude at no load, and m_x and n_x are the negative droop coefficients included for representing the gradual, negatively tilting gradients shown in Fig. 2. The droop coefficients should rightfully be tuned according to (2), to make the sources share the load demand in proportion to their ratings $S_{a,x}$

$$\begin{aligned} m_1 S_{a,1} &= m_2 S_{a,2} = \cdots = m_x S_{a,x} \\ n_1 S_{a,1} &= n_2 S_{a,2} = \cdots = n_x S_{a,x}. \end{aligned} \tag{2}$$

Upon reaching steady state, the network will have only one prevailing frequency represented by the single dashed horizontal line drawn in Fig. 2(a). At that frequency, the sum of active powers from all sources will nicely meet the total demand requested by the loads. The fractional contribution of active power produced by each source will also be in close agreement with its rating normalized by the total capacity of the subgrid, as intended. This is, however, not the case for reactive power sharing, where different line impedances between the sources and point of common coupling (PCC) commonly cause the source voltage amplitudes to be different [13], [14]. Differences can also be caused by other system mismatches, which when shifted to Fig. 2(b), correspond to those two dashed horizontal lines drawn. Such differences cause reactive power sharing to be parameter dependent, and deviate slightly from the intended.

Methods for compensating the deviation have already been explored, and can be found in [14]–[16]. They are, therefore, not further discussed here. Rather, the intention here is more focused on active power sharing between the ac and dc subgrids through the interlinking converters. Reactive power sharing wise for the formed hybrid microgrid is not as complex since it does not flow in the dc subgrid. Its sharing is, therefore, within the ac subgrid only based on the same reactive droop equation written in (1). Discussion about the interlinking converters is presented shortly after showing how active power droop control can be applied to the dc subgrid.

B. Droop Control for a DC Subgrid

Comparing with an ac subgrid, a dc subgrid is simpler with no reactive power, frequency, and phase considerations. The only quantities of interest are the active power $P_{d,y}$ and voltage magnitude $V_{d,y}$, where subscript y represents the source unit number in the dc subgrid. These two quantities, when related by (3), form the droop equation for the dc subgrid [17]

$$V_{d,y}^* = V_{d,y}' + \upsilon_y P_{d,y} \tag{3}$$

where $V_{d,y}'$ represents the maximum source output voltage under no load condition and υ_y represents the droop coefficient. When applied to more sources, (3) roughly (not precisely) leads to proportional active power sharing if their droop coefficients are tuned according to (4), where $S_{d,y}$ represents the kVA rating of source unit y

$$\upsilon_1 S_{d,1} = \upsilon_2 S_{d,2} = \cdots = \upsilon_x S_{d,x}. \tag{4}$$

An example, showing how (3) operates, is given in Fig. 3 for the simple case of two dc sources. Unlike in an ac subgrid where a single steady-state frequency prevails, voltage magnitudes of the dc sources are usually different caused mainly by parameter mismatches and finite line impedances between them and the PCC. The differences cause power sharing among the sources to deviate slightly from the intended proportional distribution just like reactive power sharing in an ac subgrid. Techniques for improving dc source sharing can, therefore, be borrowed from those for ac reactive power sharing, which supposedly are more established [14]–[16].

IV. Interlinking Control Between Subgrids

Upon knowing how to share powers proportionally among sources within each subgrid, the follow-up requirement is to coordinate among the subgrids. That must be done before power sharing can be expanded to the whole hybrid microgrid, regardless of whether the sources are placed in the ac or dc subgrid. Advantages linked to such wider scope of power sharing can broadly be summarized as follows:

1) no single point of failure introduced by an overstressed source located somewhere in the hybrid microgrid even with no fast communication link among the sources;

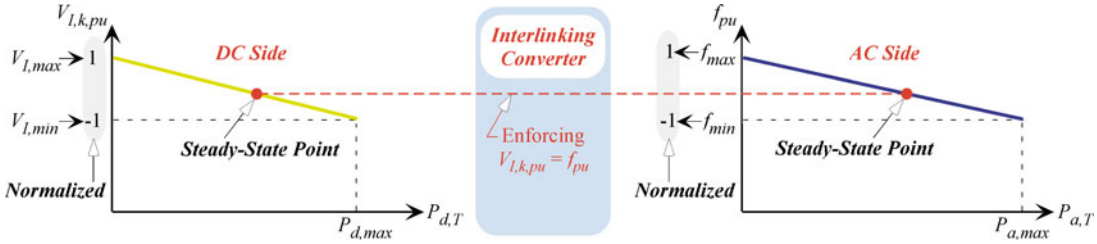

Fig. 4. Illustration of proportional power-sharing process realized within a hybrid microgrid.

2) individual source variations are always kept small regardless of where the load transients are triggered. Smaller variations might be preferred by certain sources like fuel cells, whose responses are usually slow, and therefore should not be changed too greatly, where possible;
3) source capacities can be shared between the two types of subgrids, hence allowing back-up reserve within each subgrid to be reduced considerably.

These advantages cannot be realized by just relying on the droop-controlled sources. Emphasis must equally be given to the interlinking converters, whose responsibility is to link the two types of subgrids together in a properly managed manner. Such interlinking control is presently not yet investigated, and definitely more challenging because of the following reasons:

1) Unlike unidirectional sources, the interlinking converters have to manage bidirectional active power flow between the two types of subgrids, where positive and negative polarities mean forward dc–ac and reverse ac–dc energy flows, respectively.
2) At any one instant, the interlinking converters have two roles to fulfill. They appear as sources to one subgrid where energy is injected, and appear as loads to the other subgrid where energy is taken.
3) There exist two different sets of droop equations for merging before arriving at the final active power command to be transferred by the interlinking converters for proportional active power sharing.

The aforementioned complexities can be managed by a normalization process proposed here, from which an appropriate droop control scheme for controlling the interlinking converters is developed. Underlying principles of this new droop control scheme can better be understood by referring to the example drawn in Fig. 4. In that figure, the lines drawn are for representing the combined droop responses of the ac and dc subgrids after summing all their respective source characteristics. Note that these combined characteristics need not be fully linear. They can be piecewise linear, depending on their constituting source characteristics. Regardless of that, the interlinking droop methodology developed hereon is not affected, and will respond equally well so long as the two subgrid characteristics are merged properly. This merging is not initially possible because of the different vertical axes labeled as frequency for the ac subgrid and voltage for the dc subgrid. It would certainly be helpful to bring them to a common per-unit range by adopting

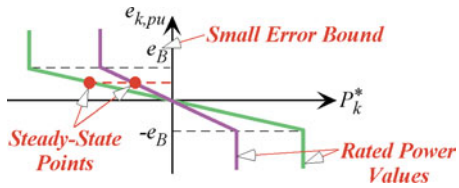

Fig. 5. Droop control scheme for cases with multiple interlinking converters between two subgrids.

those equations listed in (5) for normalization

$$f_{\mathrm{pu}} = (f - 0.5(f_{\max} + f_{\min}))/(0.5(f_{\max} - f_{\min}))$$
$$V_{I,k,\mathrm{pu}} = (V_{I,k} - 0.5(V_{I,k,\max} + V_{I,k,\min}))/ \times (0.5(V_{I,k,\max} - V_{I,k,\min})) \quad (5)$$

where V_I represents the dc terminal voltage of the interlinking converters, subscript k represents their unit number, and subscripts max and min represent the maximum and minimum allowable values of each variable, respectively.

Upon normalized, droop characteristics from both subgrids can be placed on the same plot with common vertical and horizontal axes. Criterion for proportional power sharing between the subgrids can then be inferred from earlier discussions about source power sharing, where it is noted that frequency and voltage are intentionally equalized for the ac and dc subgrids, respectively. Applying the same to the hybrid microgrid means maintaining $f_{\mathrm{pu}}=V_{I,k,\mathrm{pu}}$, corresponding to the single dashed horizontal line drawn in Fig. 4. One simple method for keeping $f_{\mathrm{pu}}=V_{I,k,\mathrm{pu}}$ is to feed their difference to a proportional-integral (PI) controller, whose output naturally corresponds to the amount of active power command P_k^* that the interlinking converters must transfer from one subgrid to the others. The eventual goal of the PI controller is to force its steady-state error to zero, which means $f_{\mathrm{pu}}=V_{I,k,\mathrm{pu}}$.

The PI approach will work well with one interlinking converter, but might deviate slightly from the ideal when multiple converters with their own PI controllers are used instead. The latter has many numerical solutions for the PI outputs, and might give different answers for different initial conditions. The same can in fact be quoted to explain why PI controllers have not been previously applied to source power sharing in an ac or dc microgrid. An alternative droop control technique is, therefore, needed for more than one interlinking converter, whose operating characteristics are better explained with the help of Fig. 5

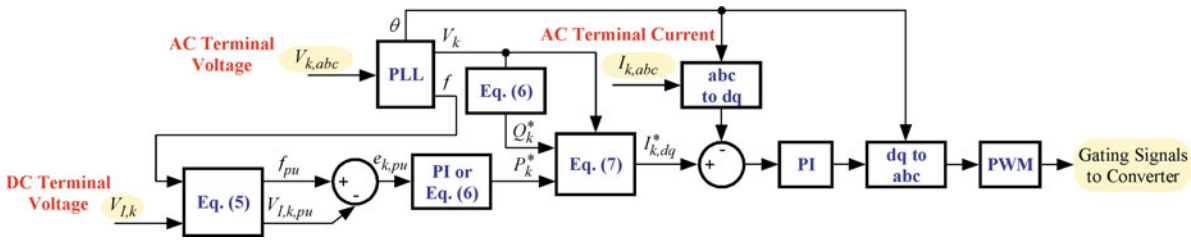

Fig. 6. Control block diagram for each six-switch interlinking converter.

for two interlinking converters. In that figure, the vertical axis represents an error calculated as $e_{k,\mathrm{pu}} = f_{\mathrm{pu}} - V_{I,k,\mathrm{pu}}$, which in the steady state is bounded by a small linear range from $-e_B$ to e_B. This error range is linearly mapped by the converter characteristics to two horizontal ranges, whose limits correspond to the respective converter power ratings.

Upon reaching steady state, the common $e_{k,\mathrm{pu}}$ detected in the ideal case will cause the two interlinking converters to transfer powers in the same direction and in proportion to their respective power ratings. Relevant operating points can be found in Fig. 5 at the same $e_{k,\mathrm{pu}}$ level. Slight deviation might however surface in practice, caused mainly by the different dc terminal voltages detected at the two interlinking converters. The difference in voltage is in turn caused by finite line impedances and parameter mismatches within the dc subgrid, which practically cannot be avoided. It is, therefore, no different from the poorer reactive power sharing experienced by the ac subgrid or in fact any existing ac grids.

Regarding reactive power, it is again emphasized here that the dc subgrid becomes "irrelevant" since it does not deal with reactive power. Reactive power control for the interlinking converters is, therefore, the same as within the ac subgrid. That means the interlinking converters use the same droop line as in Fig. 2(b) for determining their reactive power command Q_k^* from their measured ac terminal voltage V_k. However, unlike sources in the ac subgrid, Q_k^* should preferably be set to zero when active power flows from the ac to dc subgrid. Reasons for that have earlier been discussed by the authors in [27] for another topic of interest, but would still be applicable here and therefore not duplicated. Instead, it is briefly commented here that setting Q_k^* to zero during ac to dc power transfer will not be constraining since it happens when the ac subgrid is underloaded. The ac subgrid, therefore, has the ability to manage its own reactive power generation even without the assistance of the interlinking converters.

The determined power commands P_k^* and Q_k^* can eventually be written as (6) in complex form S_k^*, where γ_k is the active power coefficient for unit k. If the interlinking converters are implemented using the standard six-switch three-phase topology, S_k^* can further be substituted into (7) to get the complex current command $I_{k,dp}^*$ for tracking by the interlinking converters

$$S_k^* = P_k^* + jQ_k^*; \quad P_k^* = \gamma_k e_{k,pu};$$
$$Q_k^* = \begin{cases} n_k^{-1}(V_k - V_k') & \text{for } P_k^* \geq 0 \\ 0 & \text{for } P_k^* < 0 \end{cases} \tag{6}$$
$$I_{k,dq}^* = I_{k,d}^* + jI_{k,q}^* = 2(P_k^* - Q_k^*)/3V_k. \tag{7}$$

Here, tracking is enforced by two PI controllers placed in the synchronous frame followed by a standard pulse-width modulator. Both entities are well known, and hence need no further clarification. The final control block diagram assembled for each interlinking converter is shown in Fig. 6, which can, in principle, be viewed as the inverse of that applied to source power sharing within the ac or dc subgrid. Taking source control within the ac subgrid as an example, active and reactive powers at the source terminals are measured for determining reference values for its frequency and voltage magnitude. These values are then written as three-phase sinusoidal references for tracking by the source output voltage. The source, therefore, has voltage-source characteristics. In contrast, the interlinking control is realized by measuring the dc voltage and using a phase-locked loop (PLL) to detect the ac frequency and voltage magnitude. These quantities are then used to determine the active and reactive power commands, which upon processed by (7) give the current commands for tracking by each six-switch interlinking converter. Current-source, rather than voltage-source, characteristics are, therefore, exhibited by the interlinking converters.

Another concern emphasized with the proposed interlinking droop control is its requirement for small frequency and voltage deviations within the ac and dc subgrids. These are, however, basic requirements that are also demanded by sources in other individually droop-controlled ac and dc microgrids, as reviewed in Section III. Although frequency and voltage restorations have earlier been mentioned in [6], they are much slower secondary control that does not interfere with the faster primary droop control. That means initial frequency and voltage deviations are still demanded by the primary droop control. These deviations can certainly be kept small at the expense of power-sharing accuracy, which would in fact deteriorate to no sharing if the deviations are narrowed to zero.

For the interlinking control, it can also be hard to sense the terminal variables if their variation ranges are too narrow. Accuracy of the overall droop scheme will then be affected. This sensing constraint is less prominent within each subgrid since source droop control requires the sensing of wider power variations through its terminal voltages and currents. It is, therefore, important to consider the analog-to-digital (ADC) conversion and sampling requirements when designing the interlinking control. As some preliminary recommendations, a 2% voltage variation and a 5% frequency variation should be appropriate since they can each be accounted by 20 discrete steps with a 10-bit ADC and 20 kHz sampler (10 kHz switching frequency). These percentage variations are within allowed ranges documented

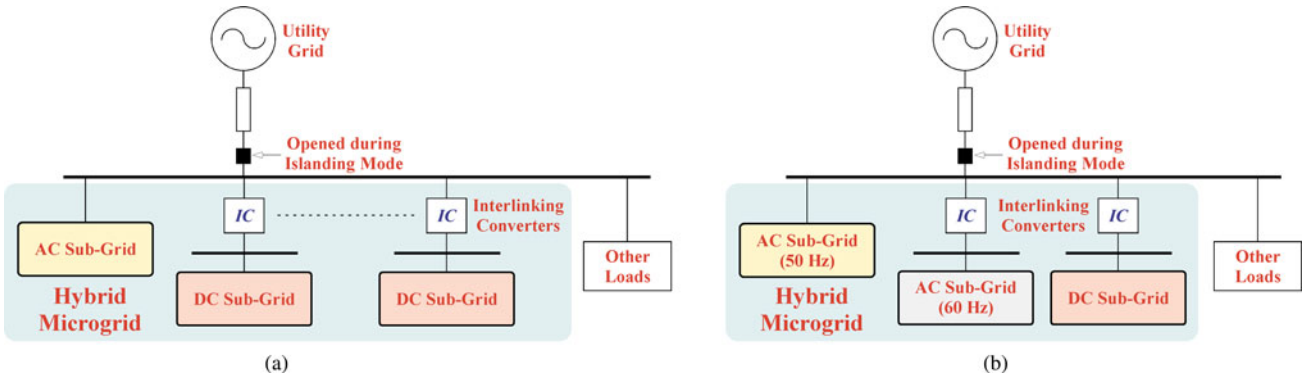

Fig. 7. Hybrid grid architectures with (a) multiple dc subgrids and (b) additional ac subgrid.

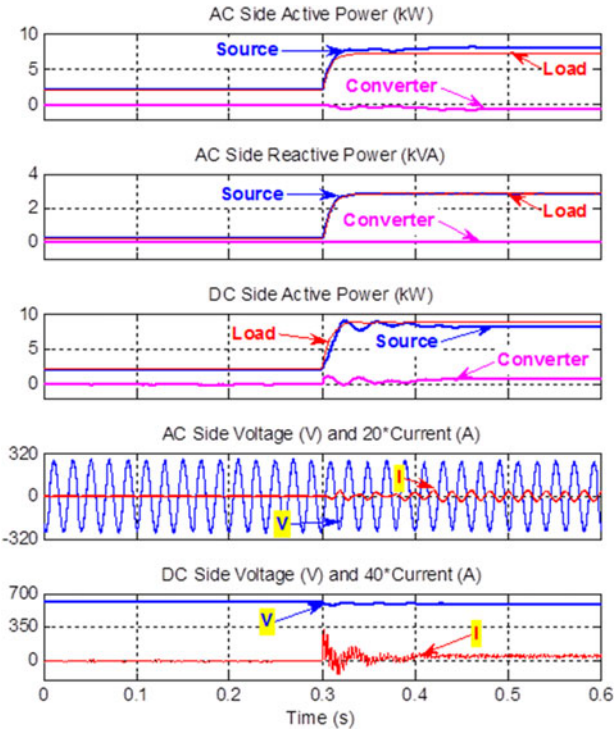

Fig. 8. Simulated ac and dc waveforms within a hybrid microgrid for the first emulated transient event.

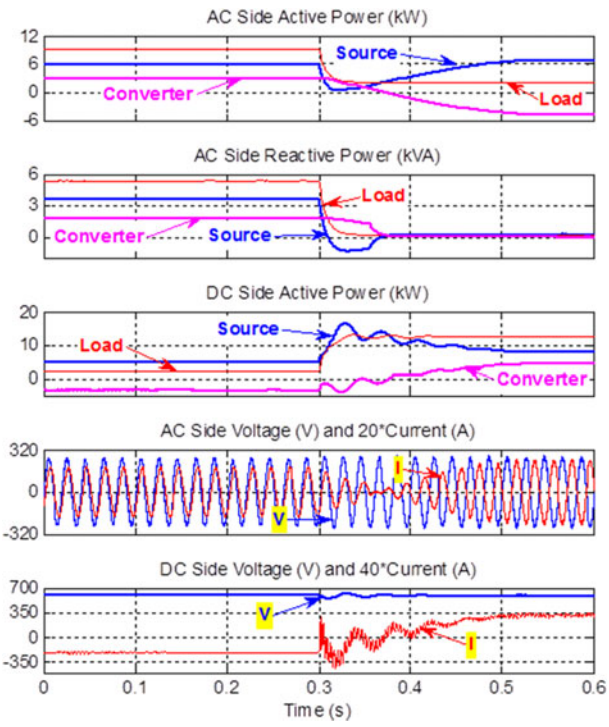

Fig. 9. Simulated ac and dc waveforms within a hybrid microgrid for the second emulated transient event.

in [28], but have to be slightly wider in practice depending on the noise level and accuracy of source sharing required by the subgrids.

V. Other Possible Grid Architectures

More complex hybrid grid architectures can be realized with more than two subgrids like in Fig. 7(a), where multiple dc subgrids are tied to the same ac subgrid through their respective interlinking converters. The dc subgrids are likely to have different voltages and variation ranges demanded by their respective local loads. Despite that, proportional power sharing throughout the whole hybrid microgrid can still be enforced by applying the proposed scheme to the interlinking converters placed between any two subgrids. The main reason why it can be achieved is attributed to the earlier explained normalization process, which upon applied will bring all subgrids to a common per-unit range for comparison like in Fig. 4. By next controlling the ac per-unit frequency and dc per-unit voltages to be equal, proportional power sharing would be enforced throughout the hybrid microgrid with each interlinking converter knowing exactly how much active power to transfer.

Other than tying dc to ac subgrid, architectures with two or more ac subgrids tied together might at times be of interest. An example is shown in Fig. 7(b), where a 50-Hz and a 60-Hz (or even higher frequency like 400-Hz) ac subgrid are linked by interlinking converters, which must now be of the direct ac–ac or indirect ac–dc–ac type. The same normalization process can still be applied to bring both subgrids to a common per-unit range for comparison. Equalizing their normalized frequencies then leads to proportional power sharing between the ac subgrids,

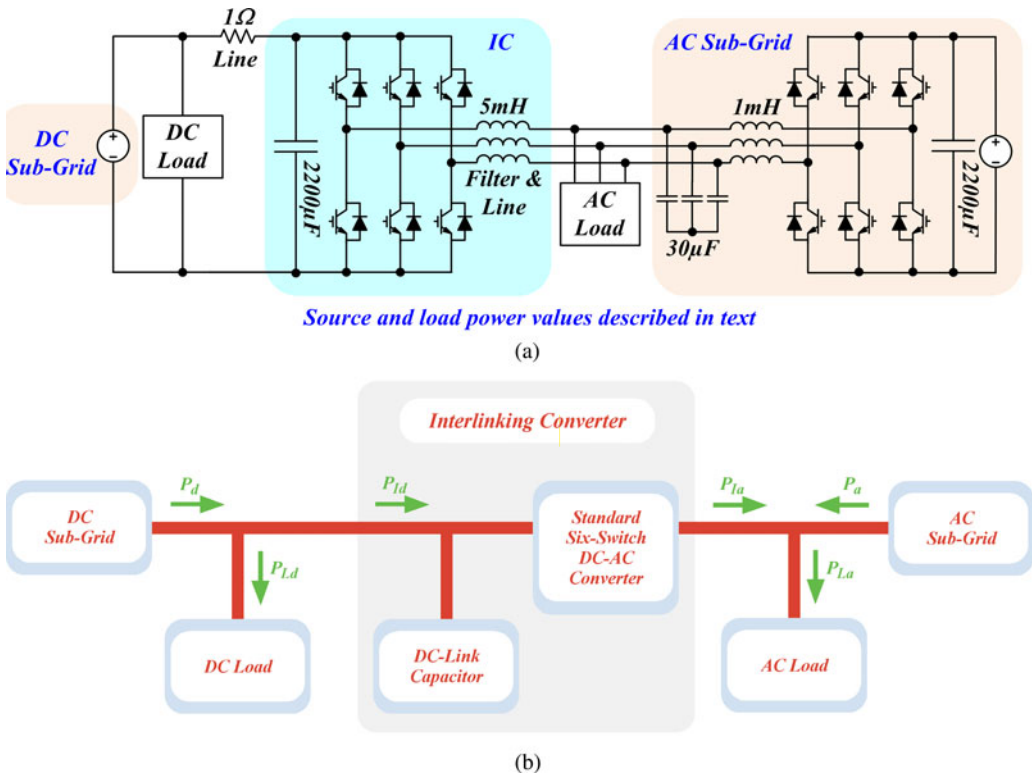

Fig. 10. Illustrations of (a) tested hybrid microgrid and (b) its reference power flow directions.

which is no different from findings discovered earlier for hybrid ac–dc microgrids.

VI. Simulation Results

For verifying its performance, MATLAB/Simulink simulation was executed with the proposed droop control scheme applied to the hybrid microgrid layout shown in Fig. 1. The total ac source ratings were 10 kW over a frequency range of 49 Hz $\leq f \leq$ 51 Hz, and 5 kVAr over an ac voltage range of 255 V $\leq V_a \leq$ 270 V. The corresponding values for the dc subgrid were 10 kW over a dc voltage range of 590 V $\leq V_d \leq$ 615 V. Since their active power ratings were chosen equal, their droop coefficients in Fig. 4 were intentionally tuned such that their generated powers were always balanced. Connecting them was two identical six-switch dc–ac converters serving as interlinking converters. They were rated at 8 kW and 2 kVAr in total, and had value of 0.05 p.u. set for e_B (see Fig. 5). When necessary, they would then transfer a maximum of 80% rated capacity from the underloaded to overloaded subgrid. Such transfer was tested for all four loading conditions organized as two transient events.

The first transient event is shown in Fig. 8, where the first three plots confirm that the two subgrids are initially experiencing a load demand of 2 kW each before $t = 0.3$ s. Reactive power demanded by the load in the ac subgrid is also read as zero during that time. Since the subgrids are equally loaded, no active power is transferred by the interlinking converters, which produce no reactive power too. These power flow observations are reinforced by the fourth and fifth plots of Fig. 8, which show voltages and currents at the ac and dc terminals of the interlinking converters. Both ac and dc currents are noted to be zero, which are certainly correct for no active power transferred. After $t = 0.3$ s, the ac and dc load demands are increased to 7.5 and 9 kW, respectively. This causes the interlinking converters to transfer 0.75 kW from the ac to dc subgrid. Because of that, source generations in both subgrids are noted to be the same at about 8.25 kW each. Reactive power generation in the ac subgrid is also noted to meet the reactive load demand exactly since the interlinking converters are not producing any during ac to dc active power transfer, as discussed in Section IV.

The second transient event is shown in Fig. 9 with its initial load conditions set to 9.5 kW and 5 kVAr for the ac subgrid, and 2.5 kW for the dc subgrid, as seen from the first three plots. Upon sensing the mismatch in active power demand, the interlinking converters help to transfer about 3.5 kW from the dc to ac subgrid. That causes their source generations to be 6 kW each, as intended. The transfer of power from the dc to ac subgrid also helps to activate reactive power control of the interlinking converters, making them share a third of the reactive load demand since their combined rating is half that of the ac subgrid. After the transient at $t = 0.3$ s, the loading conditions are reversed with the ac load demanding 2 kW and 0 kVAr, and dc load demanding 12 kW. That causes the interlinking converters to reverse their power flows with 5 kW now shifted from the ac to dc subgrid. The reversal of power and its accompanied 0 kVAr produced can also be seen from the last two plots of Fig. 9, which show terminal voltages and currents of the interlinking converters. Before $t = 0.3$ s, the ac current indeed lags the ac voltage slightly and the dc current is negative. After the transient, the ac phase difference increases to 180°, while the

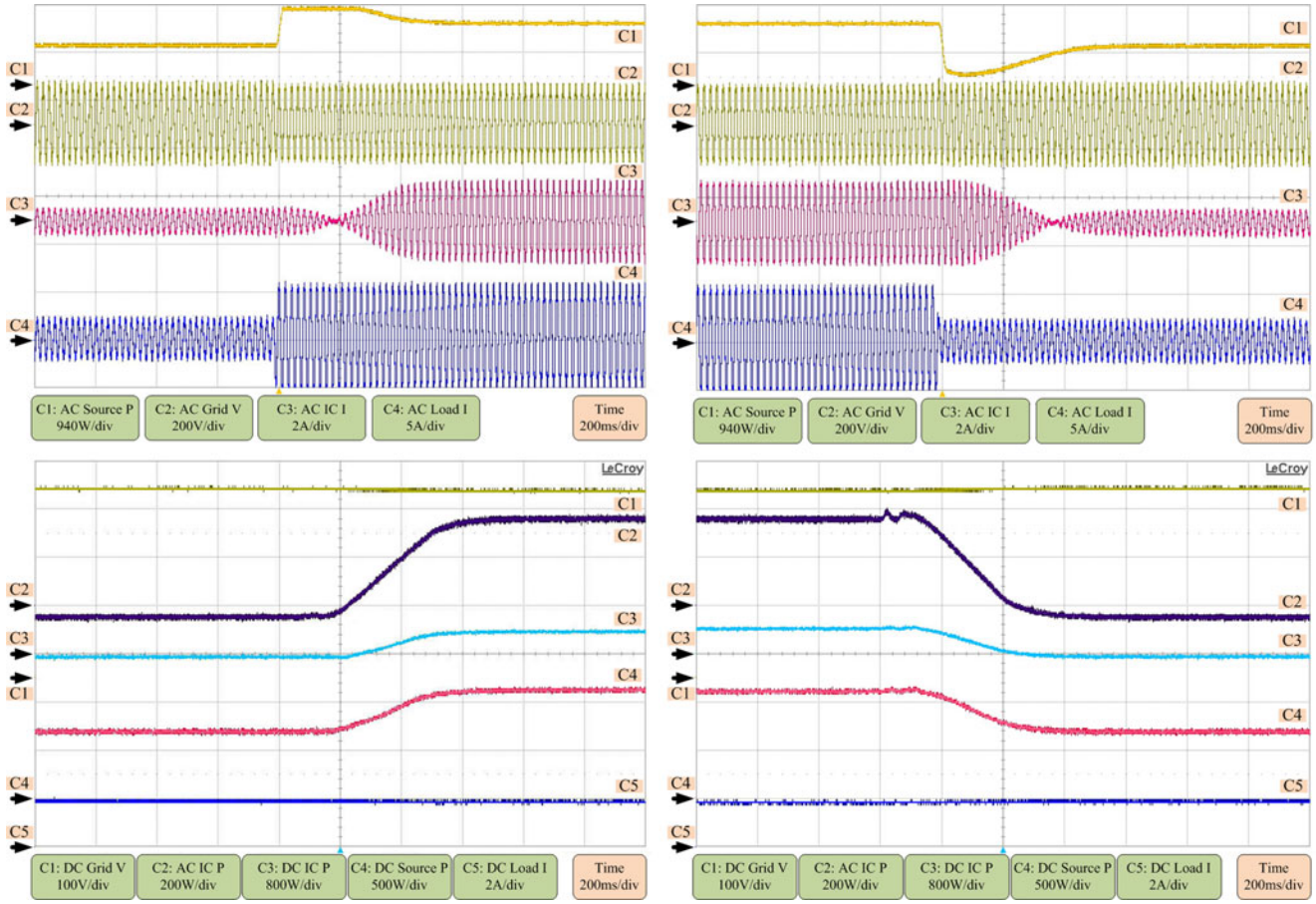

Fig. 11. Experimental ac and dc waveforms within a hybrid microgrid.

dc current rises to become positive. These certainly signify a reversal of power, which when stabilized gives rise to 7-kW source generation for each subgrid. The total load demand is, therefore, well shared within the hybrid microgrid.

VII. Experimental Results

For verifying the practicality of the proposed scheme, a scaled-down hybrid microgrid was built in the laboratory, comprising an ac subgrid and a dc subgrid [see Fig. 10(a)]. As understood from the earlier simulated plots, large amount of waveforms needed to be collected, which in practice might not be possible because of a shortage of digital scopes. Therefore, for the experimental testing, only active power flows were observed with nine waveforms captured simultaneously using two four-channel digital scopes (the ninth waveform was computed from the rest using math functions of the scopes). Observing the active power flows only was deemed as fine since the main contribution of the paper is really more to achieve proportional active power sharing for the overall hybrid microgrid.

With this objective in mind, the ac subgrid was rated at $P_{a,\max} = 1.25$ kW, $f_{\max} = 51$ Hz, and $f_{\min} = 47$ Hz (see Fig. 4 for droop characteristic), and was emulated with a separate dc–ac inverter. Corresponding values for the dc subgrid were $P_{d,\max} = 1.15$ kW, $V_{d,\max} = 400$ V, and $V_{d,\min} = 388.5$ V, and were realized with a programmable dc power supply. Note that ratings of the subgrids were intentionally set different here to demonstrate their equally satisfactory responses even under unequal source rated conditions. This was different from simulation, where equal source ratings were tried. The experimental source generations were, therefore, different, but under proportional active power sharing, their p.u. values, normalized with respect to their ratings, were always the same in the steady state. Interlinking the two subgrids was a standard six-switch dc–ac converter with a droop value of $e_B = 0.05$ p.u. and a maximum power transfer of 1 kW.

The waveforms observed are explained below, and where power quantities are concerned, their reference flow directions are indicated in Fig. 10(b).

1) *Upper plot*: C1 → ac subgrid source power (P_a), C2 → ac subgrid voltage at ac terminals of interlinking converter (labeled as IC in Fig. 11), C3 → ac current flowing out of ac terminals of interlinking converter, and C4 → ac load current.
2) *Lower plot*: C1 → dc subgrid voltage at dc terminals of interlinking converter (V_I), C2 → ac power flowing out of ac terminals of interlinking converter (P_{Ia}), C3 → dc power flowing out of dc terminals of interlinking converter (P_{Id}), C4 → dc subgrid source power (P_d), and C5 → dc load current. Under the steady-state condition, P_{Ia} and P_{Id} will be equal, but not during transient. The difference during transient is contributed by the dc-link capacitor

of the interlinking converter, which will block transient oscillation triggered by one subgrid from entering the other.

With the setup, Fig. 11 shows the experimental results with the ac and dc loads initially read as 0.72 kW (upper C4) and 0.76 kW (lower C5) at the far left of the figure. Both subgrids are, therefore, underloaded with only 0.05 kW (lower C2 and C3) transferred by the interlinking converter from the ac to dc subgrid. The resulting ac and dc source generations are read as 0.77 kW (upper C1) and 0.71 kW (lower C4), respectively, which as anticipated have the same normalized value of 0.62 p.u. At about 0.8 s later, the ac load is increased to 1.58 kW (upper C4), while the dc load remains unchanged at 0.76 kW (lower C5). If operated independently, the ac subgrid will demand for load shedding since the ac load is higher than the ac source rating by about 26.4%.

Surely, this will not happen when the subgrids are interlinked and controlled by the proposed droop scheme. Confirmation can be seen from the left set of plots, where it is shown that the interlinking converter reverses its power flow from dc to ac with 0.36 kW (lower C2 and C3) transferred in the steady state. This reversal is relatively slow since the interlinking converter must wait for the ac frequency and dc voltage to be sensed before issuing an appropriate power transfer command. During this deciding stage, the ac load increase is mostly met by an initial surge in ac source generation, which upon stabilized will reduce to a new steady-state value. Some forms of short-term storage must, therefore, be present in both subgrids to provide the transient surge in power. The new steady-state source generations are read as 1.22 kW (upper C1) for the ac subgrid and 1.12 kW (lower C4) for the dc subgrid. They again have the same normalized value of 0.97 p.u. because of the implemented proportional active power sharing.

For completeness, the right set of plots in Fig. 11 shows the reverse process with the dc load kept constant at 0.76 kW (lower C5) and ac load reduced from 1.58 to 0.72 kW (upper C4). As anticipated, the same conclusion of proportional active power sharing can be drawn before and after the load reversal, which collectively confirms the effectiveness of the proposed scheme for hybrid ac–dc microgrid control.

VIII. Conclusion

A new droop control scheme has been proposed for ensuring proportional power sharing throughout an autonomous hybrid microgrid. The microgrid is formed by tying multiple ac and dc subgrids together using interlinking converters. Through normalizing ac frequency and dc voltage, characteristic droop operating lines governing active power flows within subgrids can be brought to a common per-unit range for comparison and equalization. Upon equalized, proportional power sharing is enforced throughout the hybrid microgrid with the interlinking converters knowing precisely the amount of active power to transfer between the subgrids. Simulation and experimental results have already proven the ability of the scheme in enforcing proportional active power sharing.

References

[1] P. Chiradeja and R. Ramakumar, "An approach to quantify the technical benefits of distributed generation," *IEEE Trans. Energy Convers.*, vol. 19, no. 4, pp. 764–773, Dec. 2004.

[2] R. C. Dugan and T. E. McDermott, "Distributed generation," *IEEE Ind. Appl. Mag.*, vol. 8, pp. 19–25, Mar./Apr. 2002.

[3] R. H. Lasseter and P. Paigi, "Microgrid: A conceptual solution," in *Proc. IEEE Power Electron. Spec. Conf.*, Jun. 2004, pp. 4285–4290.

[4] H. Nikkhajoei and R. H. Lasseter, "Distributed generation interface to the CERTS microgrid," *IEEE Trans. Power Del.*, vol. 24, no. 3, pp. 1598–1608, Jul. 2009.

[5] R. H. Lasseter, "MicroGrids," in *Proc. IEEE Power Eng. Soc.*, 2002, pp. 305–308.

[6] J. M. Guerrero, J. C. Vasquez, J. Matas, L. G. de Vicuna, and M. Castilla, "Hierarchical control of droop-controlled ac and dc microgrids—A general approach toward standardization," *IEEE Trans. Ind. Electron.*, vol. 58, no. 1, pp. 158–172, Jan. 2011.

[7] J. M. Guerrero, L. Hang, and J. Uceda, "Control of distributed uninterruptible power supply systems," *IEEE Trans. Ind. Electron.*, vol. 55, no. 8, pp. 2845–2859, Aug. 2008.

[8] K. D. Brabandere, B. Bolsens, J. V. D. Keybus, A. Woyte, J. Driesen, and R. Belmans, "A voltage and frequency droop control method for parallel inverters," *IEEE Trans. Power Electron.*, vol. 22, no. 4, pp. 1107–1115, Jul. 2007.

[9] M. Prodanovic and T. C. Green, "High-quality power generation through distributed control of a power park microgrid," *IEEE Trans. Ind. Electron.*, vol. 53, no. 5, pp. 1471–1482, Oct. 2006.

[10] M. N. Marwali, J. W. Jung, and A. Keyhani, "Control of distributed generation systems: Part II. Load sharing control," *IEEE Trans. Power Electron.*, vol. 19, no. 6, pp. 1551–1561, Nov. 2004.

[11] T. L. Lee and P. T. Cheng, "Design of a new cooperative harmonic filtering strategy for distributed generation interface converters in an islanding network," *IEEE Trans. Power Electron.*, vol. 22, no. 5, pp. 1919–1927, Sep. 2007.

[12] R. Majumder, A. Ghosh, G. Ledwich, and F. Zare, "Load sharing and power quality enhanced operation of a distributed microgrid," *IET Renew. Power Gener.*, vol. 3, no. 2, pp. 109–119, Jun. 2009.

[13] A. Tuladhar, H. Jin, T. Unger, and K. Mauch, "Control of parallel inverters in distributed ac power systems with consideration of line impedance effect," *IEEE Trans. Ind. Appl.*, vol. 36, no. 1, pp. 131–137, Jan./Feb. 2000.

[14] J. M. Guerrero, L. G. Vicuña, J. Matas, M. Castilla, and J. Miret, "Output impedance design of parallel-connected UPS inverters with wireless load-sharing control," *IEEE Trans. Ind. Electron.*, vol. 52, no. 4, pp. 1126–1135, Aug. 2005.

[15] R. Majumder, B. Chaudhuri, A. Ghosh, R. Majumder, G. Ledwich, and F. Zare, "Improvement of stability and load sharing in an autonomous microgrid using supplementary droop control loop," *IEEE Trans. Power Sys.*, vol. 25, no. 2, pp. 796–808, Jul. 2010.

[16] Y. Mohamed and E. F. El-Saadany, "Adaptive decentralized droop controller to preserve power sharing stability of paralleled inverters in distributed generation microgrids," *IEEE Trans. Power Electron.*, vol. 23, no. 6, pp. 2806–2816, Nov. 2008.

[17] B. K. Johnson, R. H. Lasseter, F. L. Alvarado, and R. Adapa, "Expandable multiterminal dc systems based on voltage droop," *IEEE Trans. Power Del.*, vol. 8, no. 4, pp. 1926–1932, Oct. 1993.

[18] C. Meyer, M. Höing, A. Peterson, and R. W. De Doncker, "Control and design of dc-grids for offshore wind farms," *IEEE Trans. Ind. Appl.*, vol. 43, no. 6, pp. 1475–1482, Nov./Dec. 2007.

[19] F. Mura, C. Meyer, and R. W. De Doncker, "Stability analysis of high-power dc grids," *IEEE Trans. Ind. Appl.*, vol. 46, no. 2, pp. 584–592, Mar./Apr. 2010.

[20] M. E. Baran and N. R. Mahajan, "DC distribution for industrial systems: Opportunities and challenges," *IEEE Trans. Ind. Appl.*, vol. 39, no. 6, pp. 1596–1601, Nov./Dec. 2003.

[21] A. Sannino, G. Postiglione, and M. H. J. Bollen, "Feasibility of a DC network for commercial facilities," *IEEE Trans. Ind. Appl.*, vol. 39, no. 5, pp. 1499–1507, Sep./Oct. 2003.

[22] D. Salomonsson and A. Sannino, "Low-voltage dc distribution system for commercial power systems with sensitive electronic loads," *IEEE Trans. Power Del.*, vol. 22, no. 3, pp. 1620–1627, Jul. 2007.

[23] H. Kakigano, Y. Miura, and T. Ise, "Low-voltage bipolar-type dc microgrid for super high quality distribution," *IEEE Trans. Power Electron.*, vol. 25, no. 12, pp. 3066–3075, Dec. 2010.

[24] T. Wu, K. Sun, C. Kuo, and C. Chang, "Predictive current controlled 5-kW single-phase bidirectional inverter with wide inductance variation for dc-microgrid applications," *IEEE Trans. Power Electron.*, vol. 25, no. 12, pp. 3076–3084, Dec. 2010.
[25] H. Zhang, F. Mollet, C. Saudemont, and B. Robyns, "Experimental validation of energy storage system management strategies for a local dc distribution system of more electric aircraft," *IEEE Trans. Ind. Electron.*, vol. 57, no. 12, pp. 3905–3916, Dec. 2010.
[26] C. Jin, P. C. Loh, P. Wang, Y. Mi, and F. Blaabjerg, "Autonomous operation of hybrid ac–dc microgrids," in *Proc. IEEE Int. Conf. Sustain. Energy Techno.*, Dec. 2010, pp. 1–7.
[27] P. C. Loh and F. Blaabjerg, "Autonomous control of distributed storages in microgrids," in *Proc. IEEE Int. Conf. Power Electron. and ECCE Asia*, May/Jun. 2011, pp. 536–542.
[28] W. Christiansen and D. T. Johnsen, "Analysis of requirements in selected grid codes," DTU, Tech. Rep., 2006

Poh Chiang Loh (S'01–M'04–SM'12) received the B.Eng. degree (Hons.) and the M.Eng. degree from the National University of Singapore, Singapore, in 1998 and 2000, respectively, and the Ph.D. from Monash University, Melbourne, Vic., Australia, in 2002, all in electrical engineering.

During the summer of 2001, he was a Visiting Scholar with the Wisconsin Electric Machine and Power Electronics Consortium, University of Wisconsin-Madison, where he was involved in the synchronized implementation of cascaded multilevel inverters, and reduced common-mode carrier-based and hysteresis control strategies for multilevel inverters. From 2002 to 2003, he was a Project Engineer with the Defence Science and Technology Agency, Singapore, managing defence infrastructure projects and exploring new technology for defence applications. From 2003 to 2009, he was an Assistant Professor with the Nanyang Technological University, Singapore, and since 2009, he has been an Associate Professor at the same university. In 2005, he has been a Visiting Staff first at the University of Hong Kong, and then at Aalborg University, Aalborg, Denmark. In 2007 and 2009, he again returned to Aalborg University first as a Visiting Staff working on matrix converters and the control of grid-interfaced inverters, and then as a Guest Member of the Vestas Power Program.

Dr. Loh has received two third paper prizes from the IEEE-IAS IPCC committee in 2003 and 2006, and he is now serving as an Associate Editor of the IEEE TRANSACTIONS ON POWER ELECTRONICS.

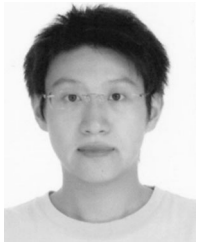

Ding Li received the B.Sc. degree in electrical engineering from Wuhan University, Wuhan, China, in 2007, and the M.Sc. and Ph.D. degrees in power engineering from the Nanyang Technological University, Singapore, in 2008 and 2012, respectively.

From July to October in 2009, he was a Visiting Scholar with the Institute of Energy Technology, Aalborg University, Aalborg, Denmark. His research interests include multilevel inverters, z-source inverters, current source inverters, and renewable energy interfacing technology.

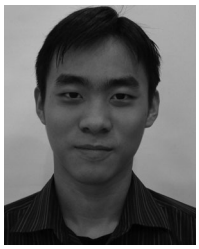

Yi Kang Chai received the B.Eng. degree in electrical and electronic engineering from the Nanyang Technological University, Singapore, in 2012.

He is currently an Engineer with SP PowerGrid Limited, Singapore, where he was involved in the operations and maintenance of high-voltage distribution switchgears, transformers, and cables.

Frede Blaabjerg (F'03) received the Ph.D. degree from Aalborg University, Aalborg, Denmark, during 1988–1992.

He was with ABB-Scandia, Randers, Denmark, from 1987 to 1988. He became an Assistant Professor in 1992, an Associate Professor in 1996, and a Full Professor in power electronics and drives in 1998 at Aalborg University. He has been a Part-Time Research Leader at Research Center Risoe in wind turbines. During 2006—2010, he was the Dean of the Faculty of Engineering, Science, and Medicine and became a Visiting Professor at Zhejiang University, Zhejiang, China, in 2009. His research interests include power electronics and its applications such as wind turbines, PV systems, and adjustable speed drives.

Dr. Blaabjerg has been the Editor in Chief of the IEEE TRANSACTIONS ON POWER ELECTRONICS since 2006. He was a Distingueshed Lecturer for the IEEE Power Electronics Society during 2005–2007 and for the IEEE Industry Applications Society during 2010–2011. He received the 1995 Angelos Award for his contribution in modulation technique and the Annual Teacher prize at Aalborg University. In 1998, he received the Outstanding Young Power Electronics Engineer Award from the IEEE Power Electronics Society. He has received ten IEEE Prize paper awards and another prize paper award at PELINCEC Poland 2005. He received the IEEE PELS Distingueshed Service Award in 2009 and the EPE-PEMC 2010 Council award.